AGU100 ADVANCING EARTH AND SPACE SCIENCE

Earth's Future

RESEARCH ARTICLE
10.1029/2018EF000820

Special Section:
The Arctic: An AGU Joint Special Collection

Increasing Arctic Sea Ice Albedo Using Localized Reversible Geoengineering

L. Field[1,2], D. Ivanova[3], S. Bhattacharyya[3], V. Mlaker[3], A. Sholtz[1], R. Decca[1,2], A. Manzara[1], D. Johnson[1], E. Christodoulou[1], P. Walter[1,2], and K. Katuri[1]

[1]Ice911 Research, Menlo Park, CA, USA, [2]Electrical Engineering, Stanford University, Stanford, CA, USA, [3]Climformatics, Inc, Livermore, CA, USA

Abstract The rising costs of climate change merit serious evaluation of potential climate restoration solutions. The highest rate of change in climate is observed in the Arctic where the summer ice is diminishing at an accelerated rate. The loss of Arctic sea ice increases radiative forcing and contributes to global warming. Restoring reflectivity of Arctic ice could be a powerful lever to help in the effort to limit global warming to 1.5°C. Polar ice restoration should be considered in planning of 1.5°C pathways. In this paper, a novel localized surface albedo modification technique is presented that shows promise as a method to increase multiyear ice using reflective floating materials, chosen so as to have low subsidiary environmental impact. Detailed climate modeling studying the climate impact of such a method reveals more than 1.5°C cooler temperatures over a large part of the Arctic when simulating global sea ice albedo modification. In a region north of Barents and Kara Seas temperatures have been reduced by 3°C and in North Canada by almost 1°C. Additionally, there are notable increases in sea ice thickness (20–50 cm Arctic wide) and ice concentration (>15–20% across large parts of central Arctic). These results suggest that the geoengineering technology proposed in this study may be a viable instrument for restoring Arctic ice.

Plain Language Summary This paper describes a method to preserve and restore ice in the Arctic in order to reduce the effects of climate change. This method is benign by design, developed to restore ice in the Arctic in targeted areas to build back the reflective ice that has melted over the past several decades. The aim is to restore the Arctic ice's historic function of reflecting sunlight. By applying reflective materials such as glass microspheres on young, low-reflectivity sea ice, we can protect the young ice from the summer Sun, much like a white shirt fends off the Sun for a person on a hot summer day. This way the ice may be conserved and converted over time into highly reflective multiyear sea ice. Climate modeling shows that this method can cool the Arctic significantly and can rebuild Arctic ice area and volume, hence reducing Arctic as well as global temperature rise.

Key Points:
- Arctic ice regrowth is an effective lever on global climate
- Albedo modification of sea ice is an effective method of ice preservation
- Albedo enhancements increase the sea ice area and volume and decrease the surface temperature

Supporting Information:
- Supporting Information S1

Correspondence to:
L. Field,
leslie@ice911.org;
lafield@stanford.edu

Citation:
Field, L., Ivanova, D., Bhattacharyya, S., Mlaker, V., Sholtz, A., Decca, R., et al. (2018). Increasing Arctic sea ice albedo using localized reversible geoengineering. *Earth's Future*, *6*, 882–901. https://doi.org/10.1029/2018EF000820

Received 23 JAN 2018
Accepted 14 MAY 2018
Accepted article online 21 MAY 2018
Published online 23 JUN 2018
Corrected 14 NOV 2020

This article was corrected on 14 NOV 2020. See the end of the full text for details.

1. Introduction

The rate of change in climate is much higher in the Arctic than elsewhere in the world, and as a result, the summer ice in the Arctic is diminishing at an accelerated rate (Intergovernmental Panel on Climate Change Fourth Assessment Report (IPCC AR4 (2007) et al., 2007; IPCC AR5, 2014)). Over the past few decades, roughly one half the surface area, and three fourths of the volume of ice in the Arctic, has now been lost, and what remains and is regrown each winter is now primarily young, and often first year, ice. Such a thin layer of ice transmits rather than reflects solar radiation, and melts quickly in the summer Sun. There is evidence as reported in a recent study that ice-ocean albedo feedback in the Arctic is shifting to a seasonal ice zone (Kashiwase et al., 2017).

Given the above conditions, we are quickly transitioning to what is known as "Blue Arctic" with faster thinning of Arctic sea ice pack (Overland & Wang, 2013). An extensive climate modeling study based on the present-day (business-as-usual) warming scenario suggests that there would be greater Arctic warming and sea ice loss using the latest climate model Community Earth System Model version 1 (CESM1; Community Atmospheric Model version 5, CAM5), with an ice-free summer Arctic occurring by about 2060, as opposed to about 2100 in Community Climate System Model version 4 (CCSM4; Meehl et al., 2013). The loss of sea ice in the Arctic is accelerating positive feedback to global warming. In fact, Pistone et al., 2014 reports that over 30 years of available satellite measurements, the decrease in albedo averaged over the globe corresponds to a forcing that is 25% as large as that due to the change in CO_2 during the same period.

Wadhams (2017) reports an even larger value of about 50% that is added to the radiative forcing of the planet due to greenhouse emissions by changes in albedo alone, when taking into account both Arctic snow and sea ice retreat. Thus, restoring Arctic sea ice reflectivity appears to be a necessary and powerful lever that could help in limiting warming to 1.5°C. Excluding polar ice restoration could make the 1.5°C goal impossible to achieve, so considerations of polar ice should be included in 1.5°C pathways (IPCC Special Report on Global Warming of 1.5°C (IPCC SR15, 2018)).

A wide variety of climate mitigation and restoration strategies that broadly fall under the term geoengineering have been proposed in order to slow, stop, or mitigate the effects of global temperature rise. However, it is increasingly clear that efforts focusing specifically on the Arctic may be necessary in order to meet this goal (Stroeve et al., 2012). Several strategies have been proposed for preserving Arctic sea ice including winter ice thickening by wind-powered pumps (Desch et al., 2017) and seawater brightening through hydrosols around the edges of the Arctic ice pack (Seitz, 2011). Cvijanovic et al. (2015) studied restoration of the Arctic ice via alteration of the ocean surface albedo. In that study, by keeping the ocean albedo high enough to maintain freezing temperatures they intensify the production of newly frozen ice and successfully expand the sea ice extent. The extending of the ice areal coverage is particularly important for reducing the polar amplification (accelerating the ice melt due to positive ice albedo feedback). However, their approach may not be very efficient in ice recovery since the generated young thin ice will still be highly transmissive of incoming solar radiation and will not insulate the underlying ocean as well as an otherwise thicker, brighter multiyear (MY) ice would have.

In this paper we report a low-risk, localized, and potentially reversible restoration solution of rebuilding reflective MY Arctic ice through surface ice albedo modification. The albedo modification method has been developed with small, localized field testing of various candidate materials in various locations, including a test site in the Arctic. In our effort to understand and quantify the possible impact of such an intervention, we use climate modeling to model and simulate increasing ice albedo as an intervention to preserve and restore ice in the Arctic. The scientific question that we seek to answer in this paper is whether a surface albedo enhancement on Arctic sea ice impacts the Arctic sea ice pack, and if so what are the impacts of such an intervention on the climate in the short and long terms.

The paper is organized into six sections. In section 2 we present the details of this new restoration and the methods that are adopted in deploying and testing some albedo-modifying materials. Section 3 details the climate modeling and simulation of this intervention, and in section 4 we focus on studying the results thereof. We summarize our results in section 5. Here we discuss the relevance of the results with respect to current research standards in climate modeling and geoengineering fields. We briefly discuss in section 6 the future work planned for studying specific areas to propose for targeted treatments that could be especially effective per unit area in preserving and restoring ice in the Arctic.

2. Surface Albedo Modification Materials, Field Testing Deployment Methods, Instrumentation, Results, and Feasibility

A localized surface albedo modification technique has been developed that shows promise as a method to slow Arctic melting, and as a means over time to increase MY ice using reflective floating materials, chosen so as to have low subsidiary environmental impact.

2.1. Materials: Overview

Dozens of materials have been considered and tested over the course of this research and development work, with a priority on safety, effectiveness, practicality, and reasonable cost.

The materials we have focused on most share many of the following characteristics:

1. high albedo (preferably at least as bright as fresh snow);
2. less dense than water (i.e., floatable);
3. nontoxic (fed to fish and birds by an environmental testing lab with no ill effects);
4. wettable (hydrophilic rather than hydrophobic, so the surface will not have an affinity for oil-based pollutants);
5. small diameter or thickness (allowing minimal materials usage per unit area);
6. larger than respirable range (avoiding inhalation effects and nanoparticle concerns); and
7. relatively low cost.

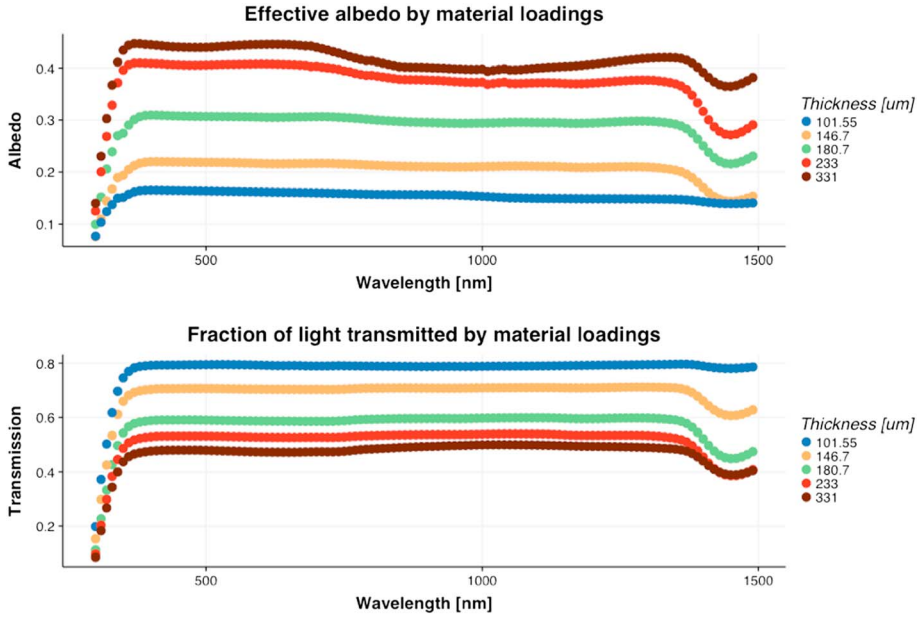

Figure 1. Laboratory testing results of (top) albedo and (bottom) light transmission for various layer thickness applications of K1 hollow glass microspheres.

There are a number of commercially available materials that fulfill some or all of the above characteristics, including some kinds of sheet-type materials, and some granular materials, including a class of commercial materials known as hollow glass microspheres. In layman's terms, these latter materials can be regarded to be chemically and physically like sand, but are floatable and round.

One of the granular materials on which Ice911 Research has done its small-scale field testing in Minnesota and in the Arctic for ice and snow preservation is K1 microspheres, a member of the 3 M Glass Bubbles family of products. This product consists of bright white hollow glass spheres, of average diameter 65 μm, chosen for its brightness, nontoxic formulation, and relatively low cost. This material has a density ranging from 0.10 to 0.14 gm/cm^3, with a typical value of 0.125 gm/cm^3, and a particle size distribution (microns, by volume) of 10th percentile: 30 μm; 50th percentile: 65 μm; and 90th percentile: 115 μm.

2.1.1. Materials: Albedo Laboratory Testing

The albedo and light transmission properties of samples of the K1 glass microsphere material were tested using ultraviolet/visible/near-infrared spectrophotometry by Covalent Metrology, an analytical laboratory. The samples were run on a Shimadzu Solid Spec 3700 DUV Spectrophotometer.

The K1 granular powder was tested at several different amounts/thicknesses, ranging from 102 to 331 μm in total, with the samples held between two glass slides. At an average granule diameter of 65 μm, these layer thicknesses cover a range from 1.5 to 5 monolayers of material, as shown in Figure 1. It can be seen in this figure that the transmission continues to be reduced and the albedo continues to increase as the thickness is increased, throughout the range tested.

2.1.2. Materials: Environmental Testing on Fish and Bird Species

The K1 material was tested by an environmental testing laboratory, EA Engineering, Science and Technology, Inc., PBC, on sheepshead minnows, *Cyprinodon variegatus*, with no ill effects.

EAG Laboratories tested the K1 material on northern bobwhites, *Colinus virginianianus*, also showing no deleterious effects.

See the supporting information Document, section S1, for further details on the environmental testing performed.

2.2. Field Testing Overview

To determine in the field how best to deploy and monitor various high-albedo materials on ice and snow, field testing in various locations was done on a small scale, with all required permits and permissions, in

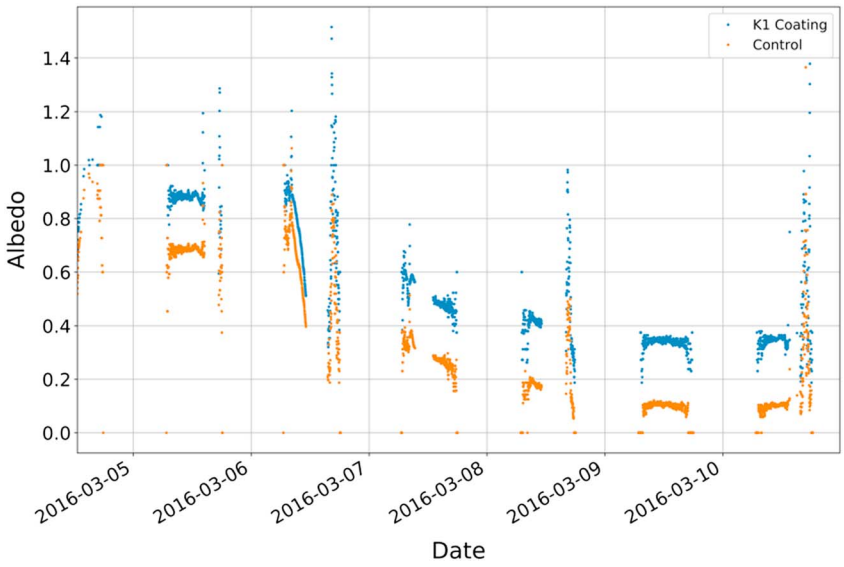

Figure 2. Albedo measurements for a control area and an area treated with K1 material, during the dates of the ice melt on the Minnesota pond in March 2016.

locations in California including Serene Lakes in the Sierra Nevada range; Lake Miquelon, a Canadian lake near University of Alberta, Edmonton; a small man-made pond in Lake Elmo, Minnesota; and North Meadow Lake, a shallow lake in the Barrow Experimental Observatory Area in Barrow, Alaska. The experience gained from the repeated seasons of experimentation in California, Minnesota, and Alaska led to improvements in the materials, instrumentation, and deployment techniques. It was found that wettable granular materials tended to be easier to maintain in place on the ice in windy outdoor conditions, especially if deployed in somewhat moist surface conditions, than sheet forms of materials. Deployment methods were developed for the granular materials for distribution by hand in very small areas, and for distribution with the aid of agricultural machinery for larger deployments on frozen lakes. The largest deployment area made by Ice911 to date was 45,000 ft^2 (4,180 m^2) of the 3 M K1 materials on a section of North Meadow Lake in Barrow, Alaska, in May 2017.

Albedo and ice preservation performance has been tracked using manual ice thickness measurements and automated cameras to record the performance of the materials and control areas, solar sensor pairs to determine albedo, strings of temperature sensors submerged in the ice and water below the instrumentation buoy, and tilt sensors. The buoys are powered by rechargeable batteries and solar panels for power. Various modes of wireless communication have been used, and data have been stored locally on SD cards in the instrumentation package on the buoy. An overview of the instrumentation challenges and strategies used in the Alaska testing was presented at a Linux conference in Europe (Chetty, 2017).

See the supporting information Document, section S2, for further details on the field testing overview.

2.2.1. Field Testing: Minnesota

Figure 2 shows the albedo measurements for a control area and an area treated with K1 material, during the time of the ice melt on a small pond in Lake Elmo, MN. Note that there are spikes in this real-life real-time data, possibly due to specular reflections from sunlight on the measured surfaces and that positioning the solar sensors can be challenging in the needed balance to ensure measurement of only the relevant area, while encompassing enough of the relevant area to be able to integrate over any heterogeneities in the surface. Throughout this time, the measurements show that the albedo values for the test area coated with the K1 are considerably higher than the untreated control area, adding 15–20% in increased reflectivity. Note that these albedo measurements are for the same areas and times shown in the automated photographs of Figure 4 taken during the ice melt.

A literature reference on transmittance and albedo for thin young ice in the Arctic is shown in Figure 3 below (Taskjelle et al., 2016).

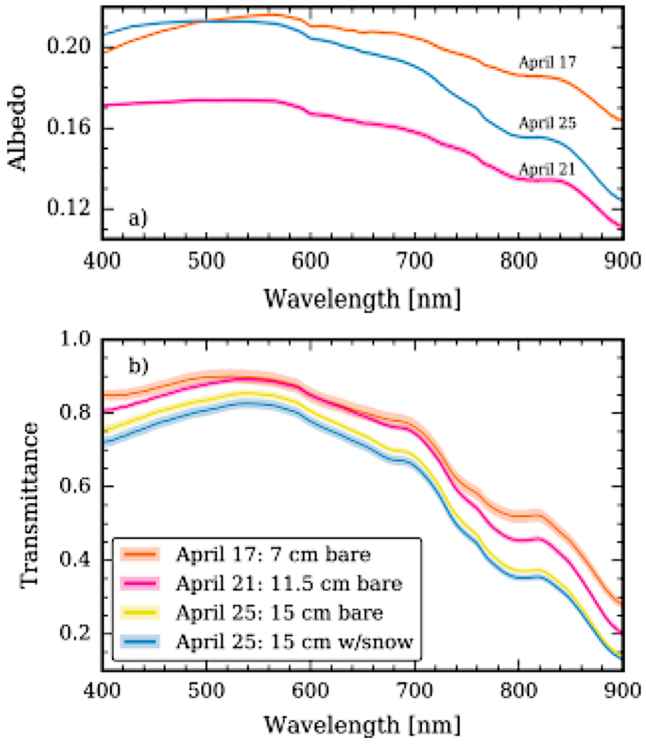

Figure 3. Measured (a) albedo and (b) transmittance for the three days. The shaded area around each line represents the ±1 standard deviation for all measurements along the transect. The number of spectra was 42, 17, 11, and 14 for 17 April, 21 April, 25 April (bare ice), and 25 April (2 mm snow cover on ice), respectively. From Taskjelle et al. (2016)

Even with a thin coating of 1.5–5 monolayers of K1 applied, the 65-μm diameter hollow glass sphere material has a higher albedo, from Figure 1, than does the 7 cm and upward of thin young ice albedo results shown in Figure 3.

Comparing Figure 3, showing albedo from field measurements of ice and snow mixtures (Taskjelle et al., 2016), with Figure 1, showing albedo from laboratory measurements of 1.5 to 5 monolayers of K1, we see that in laboratory testing, the 65-μm diameter hollow glass sphere material has a higher albedo than does the ice and snow mix.

Comparing the albedo measurements from field measurements in MN (Figure 2) with field measurements of ice and snow mixtures (Figure 3), we see that the field-tested areas treated with 5–10 monolayers of the K1 material show increased albedo as well.

Thus, in the laboratory and in the field, the treatments using hollow glass spheres contributed more reflectivity per unit thickness than the substantially thicker 7 cm ice layer of Figure 3.

To visually compare how the melt progressed in a treated and untreated areas, the photographic sequence in Figure 4 illustrates the melting in March of 2016 of one of the control areas and an area treated with K1 material on the test pond in Lake Elmo, MN. Melting and some refreezing over limited areas were underway by 5 March in parts of the treated and control areas.

By late 8 March (Figure 4b) there was a trace of ice left on one section of the control area.

With an almost identical experiment in the 2014–2015 season, on the day that the control segments completely thawed, about 3 inches (8 cm) of ice remained on the K1 treated segment, in spite of the center-edge convective circulation. (No ice thickness data is available for the day that the control segments completely thawed in the 2015–2016 season.)

In the 2013–2014 ice season (the second year of experimentation on this pond), four not-quite cubes wrapped with polyethylene film on the sides and the bottom were deployed before the pond surface froze, and after it was possible to walk on the ice, test materials were deployed. In the spring, it was observed that on the day the control section thawed completely, there was still 9″ (23 cm) of ice in the section treated with K1 glass bubbles (same application rate).

The demonstration of melting delay and of ice preservation is significant, especially when noting that the small test areas are heavily influenced by heat fluxes from the surrounding pond edges and the bottom of the pond. Consistent with this assumption were the manual measurements of a 3× increase in ice thickness observed in the 2013–2014 season (9″; 23 cm) versus the 2014–2015 season (3″; 8 cm) when the experimentation had included greater thermal isolation of each area, from the use of the plastic "cube" segmentation structure that reduced heat fluxes from other test areas, as well as the sides and the bottom of the pond.

Figure 5 illustrates that once all the ice has melted, the materials float on the water where they are blown to various obstacles, including the surrounding shore, and disappear.

Speculations are that the hollow glass spheres may be assimilated into the mud at the sides of the pond, or eventually covered by other materials leading to sinking. Less probable but possible other routes to removal of the materials are dissolution of the silica hollow walls, or possibly even breakage. The eventual fate of the materials is still being investigated in the lab and being further studied in pond testing. Intentionally, broken samples have been studied previously for any evidence of sharp edges, and to date, none have been found. The investigation is ongoing. The overall result over time from any of these routes would lead to the minimal amounts of the sand-like material that was applied (for instance, 5 to 10 monolayers of average 65-μm diameter material) being added to the local environment in the mud at the sides or bottom of the pond.

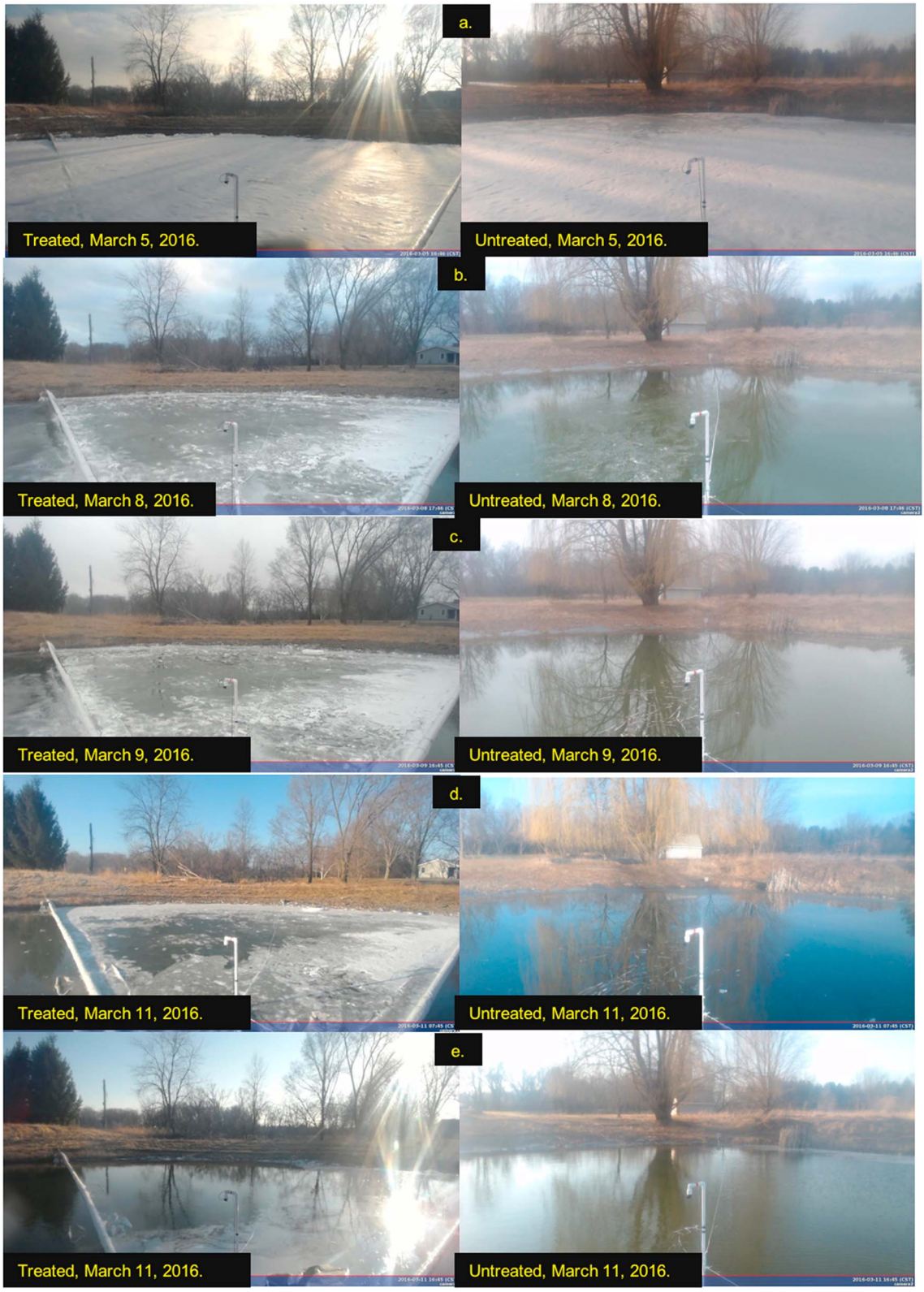

Figure 4. (a) K1-treated area (left) and one of the adjacent control areas (right), on 5 March, 2016. (b) Same areas on 8 March, when there was a trace of ice left on one section of the control area. (c) 9 March, when all ice had melted from untreated control area (right). (d) 11 March and (e) later on 11 March, when the ice, which had persisted in the treated area for several days past the disappearance of ice in the untreated control area, finished its melt throughout the day.

Figure 5. Same areas as were shown in Figure 4 (the previously K1-coated area and the control), on 15 March 2016, after the materials have dispersed.

The use of a high-albedo material, such as the glass bubbles shown here, has been shown to modify albedo and to delay ice melt. This is one of several material possibilities that Ice911 has evaluated to date. Other ice albedo modification methods, such as a proposal for ice thickening (Desch et al., 2017), may provide alternative useful means to restore Arctic ice.

See the supporting information Document, section S3, for further details on field testing in Minnesota.

2.2.2. Field Testing Deployment Methods: Alaska

Ice911's Arctic field testing has been conducted, with appropriate field testing permits, over two seasons on sections of North Meadow Lake, a shallow lake in the Barrow Experimental Observatory Area in Barrow, Alaska. The greatest progress made in this testing in Alaska has been in ruggedizing the instrumentation and developing techniques for larger-area (though still quite small-scale) deployments of the albedo-modifying test materials.

In the first season in Barrow, hollow glass spheres and similar granular materials were spread, as had been done on the pond in Minnesota, by distributing it by hand in premeasured amounts using a shaker over the test area. Localized wind shields were used to help the material settle in the desired location during application. Materials were distributed in roughly 5′ by 5′ (1.5 m × 1.5 m) areas, treated square by square to cover the total test area, as was done in Minnesota.

In the first deployment of the second season in Barrow, in March 2016–2017, the same distribution philosophy was still used, but with the addition of small portable greenhouses mounted on a pair of sleds to act as runners under opposite sides, to provide stronger and more effective localized wind shields during material application, in order to better weather the very strong winds at the site.

In May 2017, a second deployment was made, again on North Meadow Lake in Barrow, Alaska, over four areas labeled A, B, C, and D, again including K1 at two different loadings, another material, and a control area for comparison. This second deployment included the largest deployment to date by Ice911, covering an area of 45,000 ft^2 (4,180 m^2) of the 3 M K1 materials. This scaled-up, but still small test, required a move beyond manual methods.

An agricultural seed spreader was used for the deployment, donated, and customized for Ice911's application by Truax Company, Inc. (Minnesota). The machinery allowed the materials to be delivered very close to the ground while the spreader was pulled along behind a snowmobile. The deployment area was shielded from the wind by flexible plastic sheeting attached to the spreader, segmented to add to the ability to follow the ground contours. The spreader was used to distribute various types of granular glass microspheres over several neighboring test areas on the pond. A thickness of 5–10 monolayers of material was used in the various areas of these field tests. The materials were successfully deployed, and after deployment the applications of granular materials seemed to be stable in the face of local wind and storms.

The ability of the materials to remain in place once applied, in the face of Arctic wind conditions, will be an important factor to monitor in further field work and observation. Because the materials are wettable, if they are applied when there is moisture present on the surface, they have a tendency to remain where they have been placed, held by the water and eventually frozen into the ice.

Various mechanical and communications problems precluded the quantitative data gathering on the 2017 field work in Barrow, Alaska. To address this, the Ice911 team has recently placed improved monitoring and communications equipment at the same location used in 2017, North Meadow Lake, to aid in rerunning the testing.

See the supporting information Document, section S4, for further details on field testing deployment methods used in Alaska.

2.3. Feasibility Study

Questions of practicality and feasibility are critically important in the development of the ice restoration solution detailed in this study. Our aim over time is to determine the most effective locations for placements of targeted and limited applications of materials in strategic locations. Such limited, targeted deployments would be desirable in terms of costs and logistics, rather than broader deployments, and are more likely to gain the required permits and permissions. It is thought that such applications in areas such as the Fram Strait to reduce ice export from the Arctic, and the Beaufort Gyre to rebuild the circulating MY ice, are likely to be particularly strategic areas for such treatments. An outline of costs and strategies for a deployment plan for a targeted treatment in the Beaufort Gyre is given in this section. Many more details can be found in the accompanying supporting information document.

2.3.1. Production and Cost of Microspheres

Current world demand for glass microspheres stands at approximately 68,000 t/year. A deployment of 25,000 km^2 of microspheres, for example, at an average diameter of 65 μm and an applied layer thickness of 1 monolayer, or 65 μm, would require approximately 300,000 t of microspheres, which would consume world production by 2.2×. This materials demand necessitates a current microspheres producer to expand output, or for the deploying organization to build its own production facility. The production of 300,000 t of microspheres would cost approximately $300,000,000 at current prices ($12,000 per km^2 of monolayer) and require a loading volume of approximately 400,000 m^3.

Based on industry data, it would take approximately 200 production lines to produce 300,000 t of microspheres in one year. The raw material required, silica, is in ample supply to produce this volume of material and is thus not a limiting factor to production at this quantity. Microsphere production facilities currently produce with demand and affirm that production can be rapidly increased to meet 300,000 t of demand given the capital for expansion.

The lowest-cost location to produce microspheres is currently in Shandong, China, where one of Ice911's microsphere suppliers can currently produce up to 45,000 t/year and has access to the seventh busiest port in the world, Qindao Port. Qindao Port is located on the Yellow Sea and has the infrastructural capacity to load a very large crude carrier (VLCC) ships with microspheres. A factory sited near railroad tracks could deliver material in 18-t rail cars directly to the port for loading on a VLCC.

2.3.2. Shipping of Microspheres to Beaufort Gyre

Once the material is loaded onto the 1–3 VLCC ships at Qindao Port, the ships follow an approximately 8,000 km trajectory to get to Prudhoe Bay/Barrow, Alaska, and the Beaufort Gyre. This trip takes approximately nine days at an average cargo carrier speed of 20 knots. Shown below is a map of the ship's ~8,000 km path. The VLCC ships can travel approximately 46,300 km without refueling, so they are able to go directly from the port in China to the Beaufort Gyre, deploy a full load of material, and go back to the port to refill. With one blower chute on the ship, deployment of the full load would take an estimated one day—meaning that the process from port departure to full deployment is less than two weeks. The relatively short deployment process allows the option to reduce capital costs by only purchasing one VLCC and having it deploy the material in three separate trips. However, three VLCCs deploying at the same time would assure the most uniform distribution of material and would not be subject to potentially large time differences between trips due to inclement weather.

The approximate cost of shipping the material from the factory to Qindao port at current Chinese rail freight prices is around $10.4 million dollars. The approximate fuel cost to send one VLCC on the 8,000 km path is $440,000 at current fuel prices.

2.3.3. Distribution of Microspheres

To achieve a nonlinear impact on global climate (with a particularly effective deployment area), we explore the idea that the glass microspheres be distributed over a strategic area of sea ice approximately 15,000 to

100,000 km^2 in the Fram Strait, to acts as a flow restrictor on Arctic ice and water currents, and/or the Beaufort Gyre, which acts as a flywheel for Arctic ice.

The optimal time of season for deployment is estimated to be in October and November during the grease ice phase of ice formation. Grease ice is the beginning phase of ice formation in which the ocean surface layer has the characteristics of a slush. New ice forms as ice frazil crystals grow in a layer of grease ice. The grease ice layer is measured to be as thick as 70 cm but is typically around 10 cm and eventually congeals into a layer of solid ice, depending on surface temperatures (Smedsrud & Skogseth, 2006). Application of the microspheres to grease ice ensures that microspheres will be applied to the top layer of what will become first-year (FY) ice, which cools the surface layer and enhances the reflectivity of FY ice as it builds from below. Moreover, application to grease ice circumvents any interaction of the material with mammals such as polar bears as it is dispersed from the deployment ship because they are unable to access grease ice.

2.3.4. Dispersal Vehicle for Material Deployment

In order to deploy microspheres in the harsh Arctic environment, various methods of material distribution in the key locations have been explored:

1. Land-based methods such as custom terrestrial spreaders have been used in Ice911's test site in Barrow, Alaska, but will not be sufficient to cover these large areas in reasonable time. The terrain on sea ice is often very nonuniform and can change rapidly, making such an operation hazardous to people and equipment as well.
2. Air-based methods, such as adapting drones, balloons, or aircraft, quickly run into limitations of loading, particularly from the large volume needed of the very lightweight materials—thus requiring considerable fuel and many flights to accomplish the job.
3. This document details the use of one or more large vessels on the ocean itself, with the range of material distribution extended by the use of blowers.

The optimal vehicle for deployment must combine long travel range, durable construction, and immense cargo volume due to the packing density of the material. Therefore, Ice911 has determined that the most feasible route to full-scale deployment is to use readily available ships. Optimizing for lowest cost, the deploying organization can buy one to three VLCC ships and adapt them for the deployment of microspheres. VLCCs are ocean tankers built to carry large volumes of cargo or liquid internationally. With cargo volumes between 150,000 and 200,000 m^3, it would take either three VLCCs or one VLCC on three separate trips to deploy 25,000 km^2 of microspheres.

See the supporting information Document, section S5, for further information strategies for materials dispersal for targeted deployment in the Beaufort Gyre.

In the next two sections, we describe the details of climate modeling of the Ice911 ice preservation and restoration technology and further study the impacts of the albedo modification material on the climate.

3. Modeling Study

A detailed modeling study is designed to simulate the potential impact of Ice911's albedo modification through added material on the Arctic sea ice, using a state-of-the-art climate model. It is aimed at investigating regional- and large-scale climate impact of changes in the Arctic sea ice albedo. We specifically seek to understand how these changes impact the distribution of the Arctic sea ice area, concentration, volume, thickness, and temperature.

We assume that the major physical effect of the Ice911 material when applied to sea ice is to increase the sea ice albedo. We investigate the effect of increasing of the Arctic sea ice albedo basin-wide by changing the model sea ice albedo everywhere where sea ice exists (both Arctic and Antarctic). This simulation will provide the extreme scenario and show the potential impact when the entire sea ice pack is treated with Ice911 material.

Our major tool is the National Center of Atmospheric Research CESM (version 1.2). This is a fully coupled global climate model, which consists of atmospheric, ocean, land, and sea ice components interacting and exchanging water and energy fluxes via coupler (CPL7; Hurrell et al., 2013). We utilize B compset, which is a present-day (2000s) greenhouse emission forcing scenario. It is configured with components CAM4,

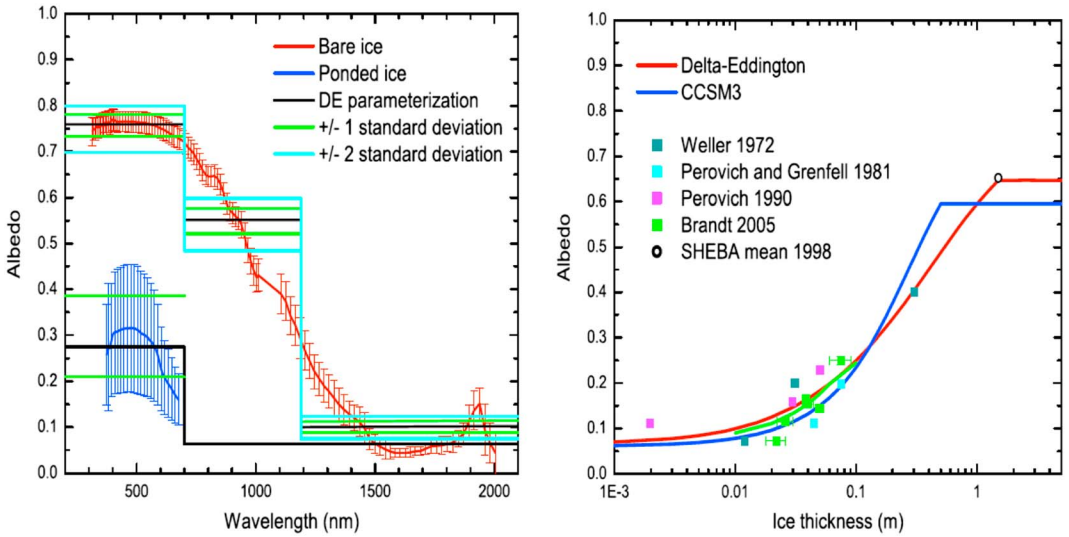

Figure 6. delta Eddington (DE) parameterized ice albedo: (a) for different wavelengths compared to observations and (b) for different ice thickness compared to observations (squares) and albedo parameterization in earlier model version CCSM3. From Briegleb and Light (2007). Copyright 2007 Bruce Briegleb and Bonnie Light. This work is licensed under a Creative Commons Attribution-Noncommercial 4.0 International License (https://doi.org/10.5065/D6B27S71).

CLM4 (Community Land Model, version 4), POP2 (Parallel Ocean Program, version2), and CICE4 (Los Alamos Sea Ice Model, version 4) onto a nominal grid resolution of 0.9 × 1.25° in the atmospheric and land model domains and 1° in the sea ice and ocean model domains.

To modify the sea ice albedo, we are using the "delta Eddington" (DE) shortwave parameterization in the sea ice model component of CESM (Briegleb & Light, 2007), which calculates the albedos and the absorption of the shortwave fluxes. Figure 6a shows the modeled ice albedos by the DE (black lines) parameterization compared to SHEBA observations of the summer of 1998 (red and blue lines). The relationship between the albedo and the ice thickness seen in Figure 6b for both observations (squares) and models (CESM-DE in red line, CCSM3 in blue line) is strongly nonlinear up to 1-m-thick ice. For 100 μm of ice, albedo is 0.07, for 300 μm about 0.008 from various researchers, and the highest albedo of about 0.65 is for 1 m of ice. The laboratory-tested value of K1 of approximately 0.45 for 330 μm of K1 as was shown previously in Figure 1 is far higher than the values of 0.008–0.07 found by various researchers for 100–300 μm of ice. In fact, the albedo of 0.45 measured or 330 μm of K1 material is closer to the values measured for over 0.2 m of ice, 600 times the thickness of the albedo enhancing material used.

There are three types of physical media considered in the sea ice model: sea ice (represented with five ice thickness categories), snow, and melt ponds. For each of them there is a separate calculation for albedo and shortwave absorption involving their optical and thermal properties, which can be changed via tunable parameters. In a series of test experiments and also previous studies (Urrego-Blanco et al., 2016) we found that the highest sensitivity of the broadband albedo is to the snow tuning parameters. By tuning the snow parameters we create the perturbations in overall broadband albedo, which we use to set up our final sensitivity experiment.

3.1. Numerical Experiments

As a starting point, a common spin-up data set is used for all simulations. This is necessary to obtain a reasonably steady stable climate state, which will provide the initial conditions for all the simulations that we need to run. After 40 years of integration the atmospheric state seems to tend to equilibrate. All of the biases in the radiative balance are reduced. The ocean takes longer to spin-up and is still adjusting at 40 years. However, as a first approximation, we use this model solution to initialize our next set of experiments.

We carried out two major experiments: (1) Control Experiment where we keep the standard settings of the model. It starts in 2000 and represents a short-term (ending in 2040) future projection of the current climate state under the 2000s greenhouse gas (GHG) forcing. (2) Global Sea Ice Albedo Experiment where we change the sea ice albedo everywhere sea ice exists (both Arctic and Antarctic). The albedo

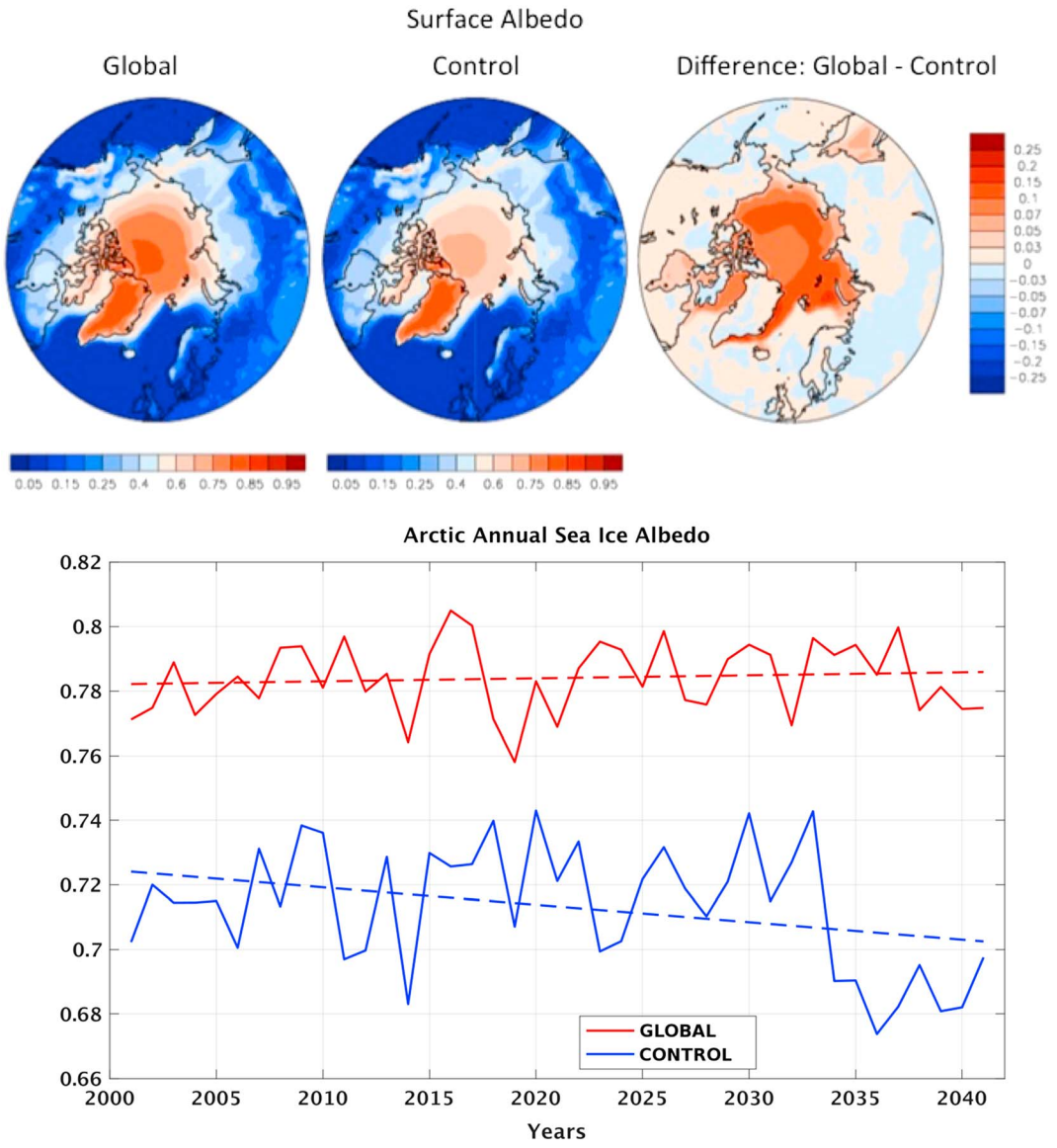

Figure 7. Arctic surface albedo perturbations: (a) Map of Arctic surface albedo for Global albedo modification of sea ice averaged over 40 simulation years. (b) Map of Arctic surface albedo for Control averaged over 40 simulation years. (c) Map of differences in surface albedo between Global albedo modification and untreated Control averaged over 40 simulation years. (d) Time series and linear trends of Arctic annual sea ice albedo for Global albedo modification (red), and untreated Control (blue).

perturbation is introduced from the beginning in 2000 and is applied continuously during the entire integration. This sensitivity experiment is representative for the application of the geoengineering ice restoration technology of Ice911 on the global sea ice pack.

The albedo perturbations, which we set up in our experimental design, are presented in Figure 7. In Figures 7a and 7b we see the mean state of the surface albedo in the Arctic area for the 40-year period of integration in the two model simulations considered in this study (Global and Control, respectively). Both spatial patterns look similar (Figures 7a and 7b) with the highest albedo values in the area of land-ice covered Greenland and over the thickest sea ice pack in central Arctic close to the Canadian Archipelago. The lowest surface albedos are found over the ocean and land, which have less reflectivity than the ice surfaces. Within the Arctic basin, the lowest albedos of 0.2–0.25 are found in the marginal ice zone rapidly increasing toward the Central Arctic up to 0.7–0.75. The albedo perturbations in the sensitivity experiment are applied only on the sea ice cover so we see the largest albedo differences between the two experiments over the Arctic sea

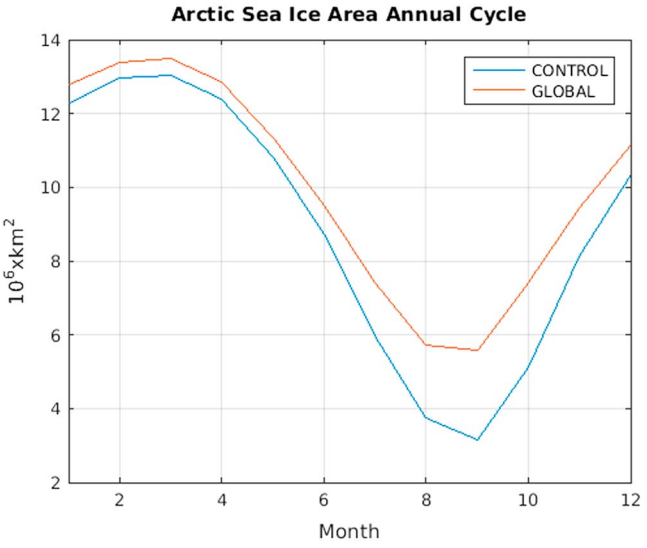

Figure 8. Annual cycle of the Arctic total sea ice area for Global albedo modification (red) and untreated Control (blue).

ice pack (Figure 7c). The Global ice albedo ranges from 0.25 to 0.8 within the Arctic basin. The strongest impact of the albedo modification is found in the marginal sea ice zone.

It may be noted that the range of values for Arctic surface albedo in our Control experiment (Figure 7b) is within the same range as the ones reported by Briegleb and Light (2007) (Figure 6). Figure 7d shows the annual time series of the average Arctic sea ice albedo and their linear trends for the two experiments. In the Control experiment (blue) we see a rapid decline of the surface albedo within the next 25 years. The latter is a consequence of the ongoing transition to "Blue Arctic" state of thinner, faster, and less compact Arctic sea ice pack (Overland & Wang, 2013). In the sensitivity experiment, Global, where the albedo modification is applied, we see a modest long-term positive trend in the sea ice albedo. The magnitude of the Arctic averaged sea ice albedo increased 10–15% compared to the Control. This modeled albedo modification is comparable to the Ice911 K1 material albedo enhancement of 15–20% in the Minnesota pond field experiment (Figure 2).

4. Modeling Results

In the following section we present the impact of the surface sea ice albedo perturbations, which we set up in the Global sensitivity experiment to simulate the effect of the Ice911 geoengineering on the Arctic sea ice area, volume, and surface temperature. We use the results from the Control experiment, projection of the current climate state under GHG 2000s forcing, to provide a baseline for comparison. Note that the only differences between the two experiments are the albedo perturbation.

4.1. Sea Ice Area and Concentration

We begin our analysis with the impacts of the albedo perturbation on the seasonal variability of the Arctic sea ice area. The total sea ice area is derived as cumulative sum of the ice-covered area of all grid cells of the model grid within the 15% contour of sea ice concentration in the northern hemisphere. It is expected that the largest effect of the enhanced albedo will be on the thinner, such as younger or melting, sea ice, due to its lower reflectivity compared to the thicker MY sea ice. The annual cycles of the total Arctic sea ice area in the two numerical experiments shown in Figure 8 reveal that the most significant increase of the ice area is during the melt season.

The seasonal maps of the sea ice concentration (Figure 9) confirm this result showing modest increase during the winter at the sea ice edge most of all in the Barents Sea (Figures 9a and 9b) and strong increase of more than 20% of the ice concentration everywhere in the Arctic marginal ice zone during the summer (Figures 9c and 9d).

The interannual variability and long-term trends of the Arctic total sea ice area are shown in Figure 10. The albedo perturbation has caused an instantaneous increase of the sea ice area during the initial period of the integration of Global experiment from 9×10^{12} to 9.7×10^{12} m^2. As anticipated for a present-day scenario, the Control case has a long-term decline of the annual total ice area. In order to compare our results to the reported in the IPCC AR5 we consider the sea ice extent, which is the overall surface area within the 15% contour of sea ice concentration. It is often preferred to the actually ice-covered area in previous studies (including IPCC AR5) due to the higher confidence in measurement and simulation. For the purposes of the current numerical study we focus on the sea ice area since that it is the actual area where the sea ice albedo perturbations are applied. In our Control experiment the September minimum of the total Arctic sea ice extent (not shown), often used as an indicator of transition to seasonal ice-free Arctic, has a decreasing trend of $\sim -0.2 \times 10^6$ km^2/decade, which is smaller than the observed -0.8×10^6 km^2/decade for the same period but within the range of the CMIP5 historical simulations (IPCC AR5, Chapter 9, Figure 9.24). In the albedo perturbation Global case we see increasing trends in both annual and September ice time series.

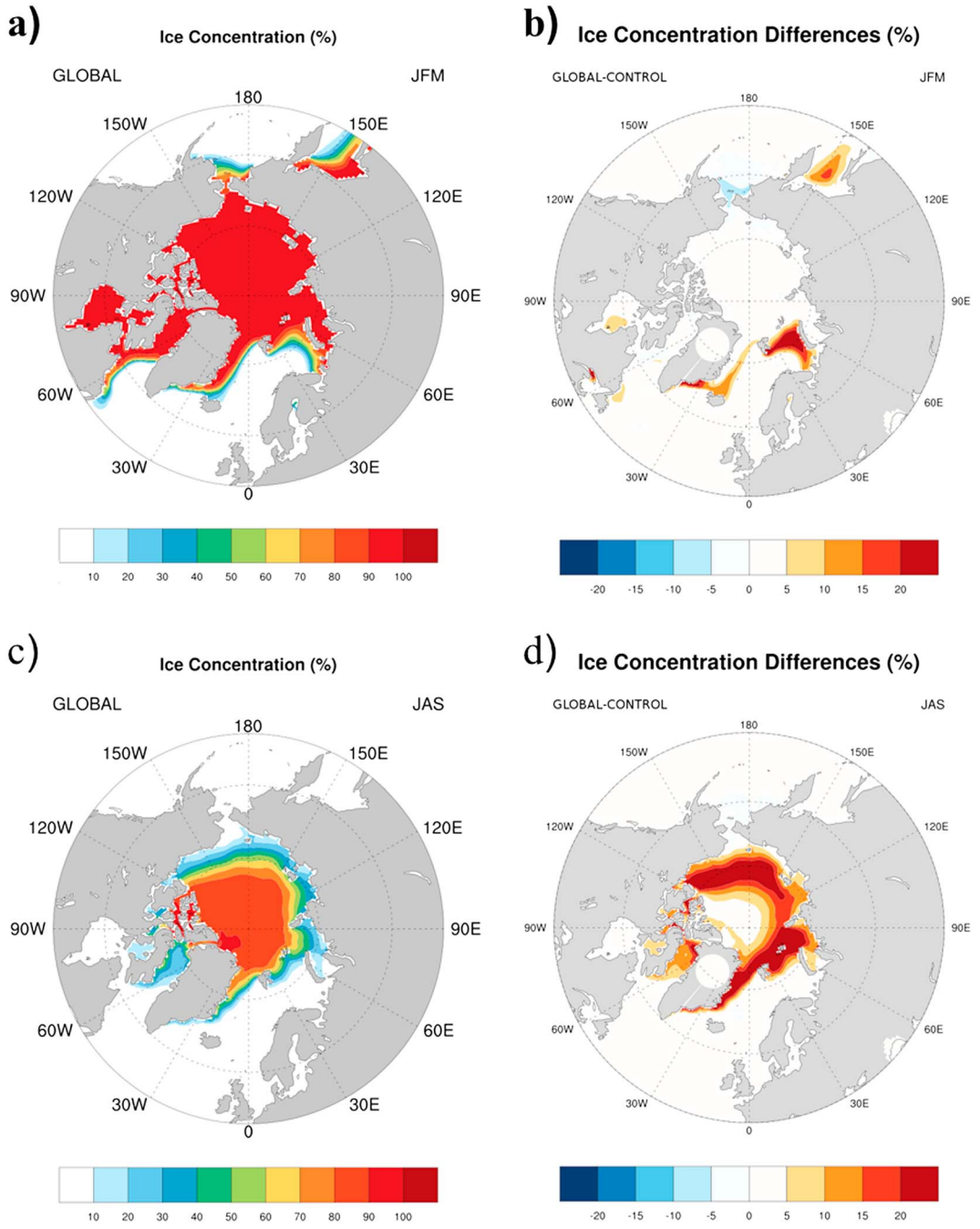

Figure 9. Sea ice concentration maps of (a) winter mean (January-February-March) for Global albedo modification; (b) difference in winter (January-February-March) mean between Global albedo modification and untreated Control; (c) summer mean (July-August-September) for Global albedo modification; (d) difference in summer mean (July-August-September) between Global albedo modification and untreated Control.

For a stable Arctic recovery it is important the FY ice to survive the melt season and transition to a MY sea ice. To see if that is the case in our albedo perturbation experiment, we investigate the ratio of MY and FY ice fraction. In Figure 11, we see that in the Control case, this ratio is decreasing, meaning that the fraction of the MY ice is reducing compared to the FY fraction. This type of FY dominant ratio suggests transitioning toward seasonal ice pack when the generated winter sea ice does not survive the following melt season. In contrast, the Global experiment shows a strong increasing trend of the MY/FY ratio proving the growth of the perennial ice fraction.

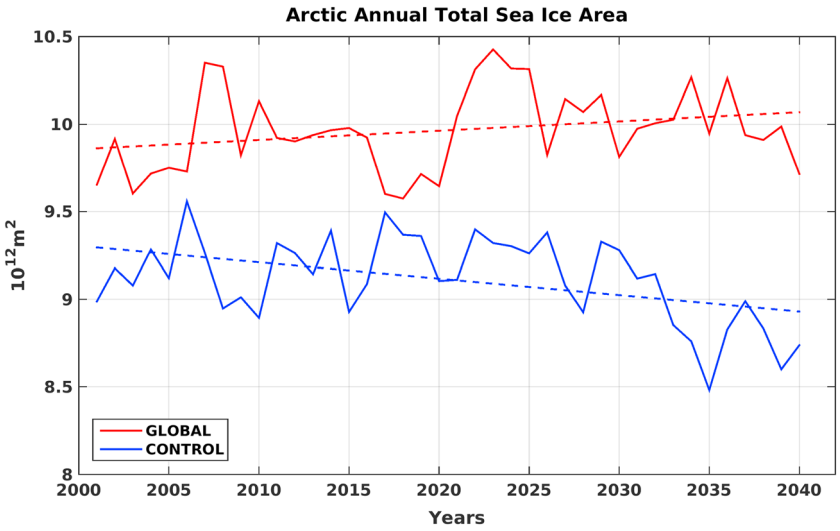

Figure 10. Time series and linear trends of Arctic annual total sea ice area for Global (red) and Control (blue).

4.2. Sea Ice Volume and Thickness Changes

The sea ice volume is a product of the sea ice area and sea ice thickness; thus, its changes reflect both the changes in the sea ice thickness and the sea ice area. To evaluate the fidelity of our Control case Arctic sea ice volume, we compare it to the Pan-Arctic Ice Ocean Modeling and Assimilation System (PIOMAS) Arctic Ice Volume Reanalysis for the period 2000–2017 (Zhang & Rothrock, 2003). PIOMAS was developed at Applied Physics Laboratory with the goals to simulate and understand the mechanisms of the current Arctic decline and project the future Arctic states under different scenarios and so far it is the only sea ice data assimilation product and closest to observational estimate available for the sea ice volume. Figure 12 shows the monthly time series of the total sea ice volume in Control and PIOMAS. Their magnitude of the seasonal cycle seems to be in a good agreement, and they, both exhibit declining trend in this period, but it is much smaller in the Control. There is a better agreement for the later period 2010–2017 where comparison of the difference in the average sea ice volume in our Control for the year 2017 is about 1,000 km^3 higher than in 2010, which is in the same order of magnitude as has been reported (1,100 km^3) in the following PIOMAS model literature http://psc.apl.uw.edu/research/projects/arctic-sea-ice-volume-anomaly/.

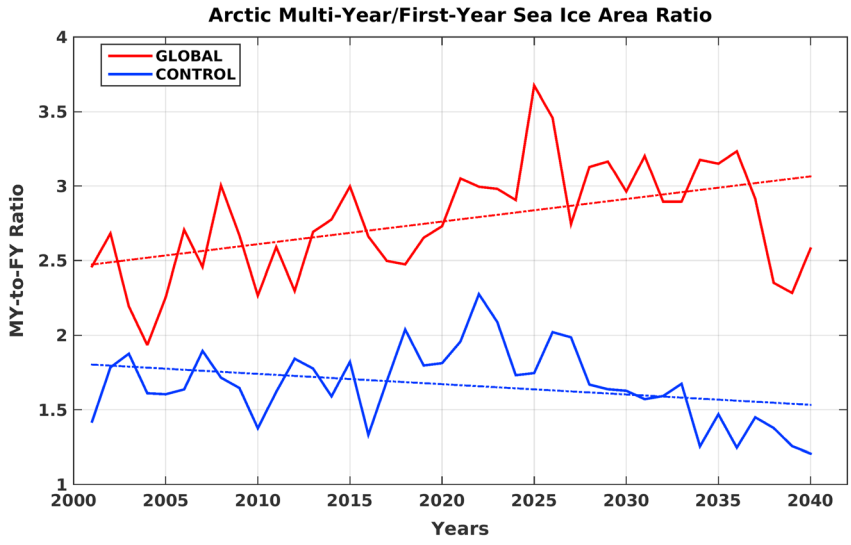

Figure 11. Time series and linear trends of the ratio between multiyear and first-year sea ice fraction in Global (red) and Control (blue).

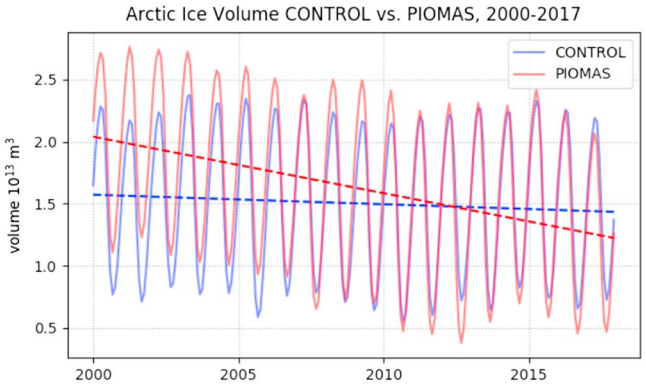

Figure 12. Time series of total Arctic sea ice volume of Control (blue) compared to PIOMAS data (red).

We compare next the annual cycles of Arctic total sea ice volume between the two numerical experiments Control and Global shown in Figure 13. Clearly, the Global albedo modification experiment shows larger total Arctic sea ice volume compared to the Control. Compared to the changes in the sea ice area where the largest impact from the albedo modification was in the summer season, the ice volume is enhanced through the entire year.

The maps in Figure 14a shows the winter mean state of the Arctic ice thickness distribution during the 40 years of integration in the two experiments. They both simulate the observed pattern of thicker ice in the Canadian Archipelago coast and Greenland, thinning toward the Siberian coast, and the marginal zones in the North Atlantic and Pacific varying in 0–5 m range. The differences between the two experiments (Figure 14b) demonstrate large-scale thickening of the ice pack in the case of increased albedo (Global exp) ranging from 20 cm up to 1 m in the Canadian Archipelago. The impact is even stronger in the summer season where the central Arctic has thickened with about 20–50 cm and gotten covered with $>$1.5-m-thick ice (Figures 14c and 14d).

The time evolution of the Arctic averaged annual sea ice volume is shown in Figure 15. In the Control (blue) we see a declining trend, which is similar to that seen in the PIOMAS sea ice volume (see Figure 12) over the period 2010–2017 (see http://psc.apl.uw.edu/research/projects/arctic-sea-ice-volume-anomaly/).The continuous application of the Ice911 material causes ice volume increase of ~0.5 to 1%/year. For the 40-year period, the Global experiment shows 6% increase per decade while the Control has 2% decrease; therefore, the albedo enhancement experiment mitigates the Arctic sea ice volume by 8% per decade.

4.3. Surface Temperature Changes

Changing the reflective properties of the sea ice will lead to changes in the Arctic energy balance, affecting the surface energy budget thus changing surface temperatures. The detailed consideration of the energy budget results is out of the scope of the current paper. Here we consider the impact of the albedo increase on the regional Arctic and world-wide global surface temperature (Figure 16). In Figure 16a, we show the maps of the surface temperature mean climatologies for the 40-year period of integration. The cooler temperatures are seen over the most reflective ice areas. The difference map in Figure 16b reveals that increasing the albedo in Global experiment is causing a decrease in the surface temperature. Over a large part of the Arctic we see more than 1.5°C cooler temperatures. In a region north of the Barents and Kara Seas temperatures have decreased by 3°C and in North Canada by almost 1°C.

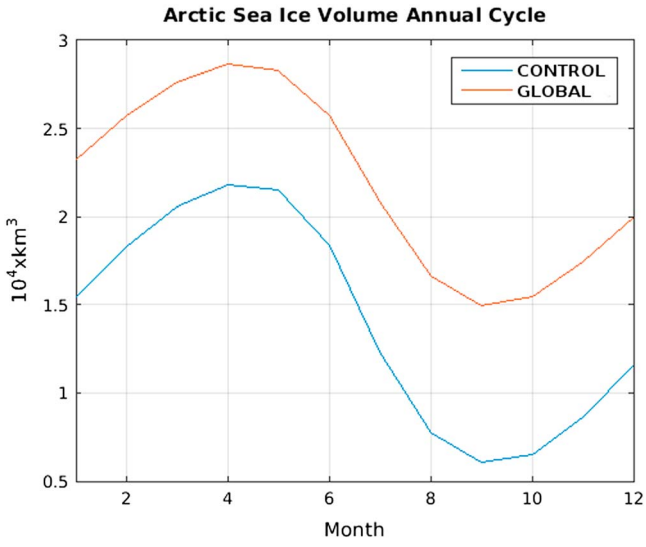

Figure 13. Annual cycle of the total Arctic sea ice volume in Global albedo modification (red) and untreated Control (blue).

Figure 17a shows a long-term declining trend of the Arctic surface temperature in the Global experiment. Such an Arctic basin-wide cooling trend in temperature over the long run may prove to be promising for Ice911's geoengineering technology, if it can indeed be tested and demonstrated: (i) at large scale, (ii) for extensive duration, and (iii) in maritime environments. So far the results are presented here only for an idealized scenario involving albedo modifications to the entire global sea ice area. Figure 17b shows a long-term warming trend of about 1°C of globally averaged surface temperature interannual anomalies for the untreated Control (blue dashed line) and a modest cooling trend of about 0.02°C for the Global albedo modification case (red dashed line), over the period 2000–2040. The Control case uses 2000 GHG forcing for each year of the simulation. We assumed that the emission level at year 2000 is not increasing with time (as if due to stricter emission enforcement already in place). The results from this scenario are similar to Representative Concentration Pathway (RCP) 2.6. This shows that over the period 2000–2040, Global albedo modification could in fact prevent the 1°C rise in average global temperature

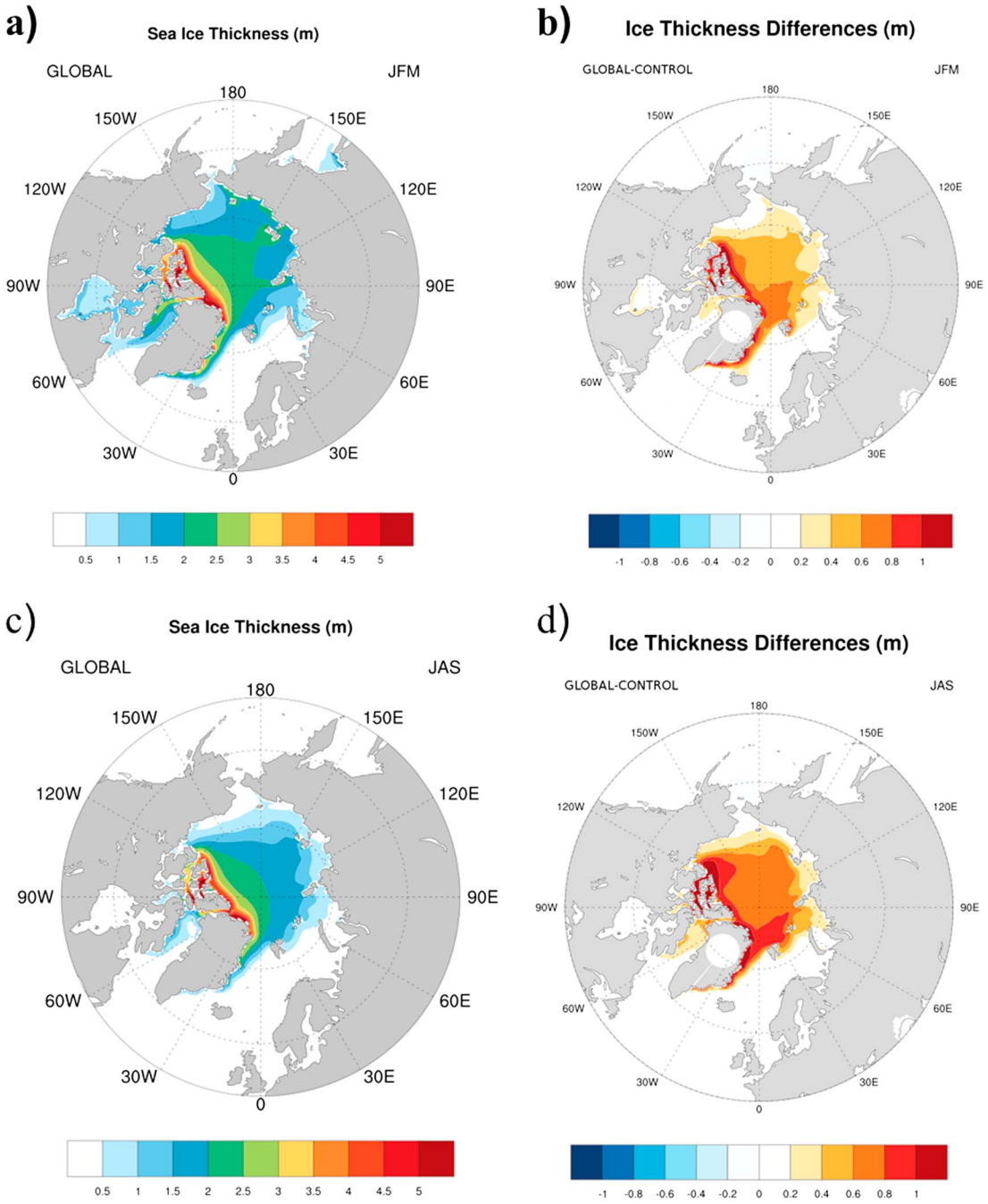

Figure 14. Sea ice thickness maps of (a) winter (January-February-March) mean for Global albedo modification; (b) difference in winter mean between Global albedo modification and untreated Control; (c) summer (July-August-September) mean for Global albedo modification; (d) difference in summer mean (July-August-September) between Global albedo modification and untreated Control.

predicted by the untreated Control, and in addition could further reduce the average global temperature by 0.02°C during the same period.

5. Conclusions and Discussions

The novel idea that this paper presents is to explore whether melting of sea ice in the Arctic can be slowed down by using a localized reversible geoengineering Arctic restoration technology that increases Arctic sea ice albedo. It addresses the scientific question of what is the impact of albedo enhancement over sea ice

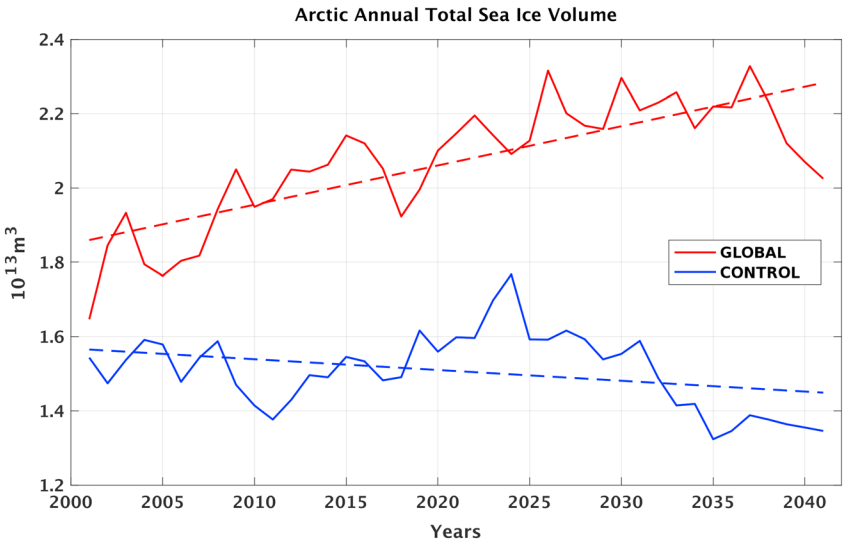

Figure 15. Time series and linear trends of the Arctic annual total sea ice volume for Global albedo modification (red) and untreated Control (blue).

particularly over the Arctic. It shows how such a modification impacts the sea ice area, sea ice volume, and temperature and demonstrates the nature of these responses.

Seasonal sea ice area shows significant increase compared to the untreated Control during the melt season. The seasonal sea ice concentration shows a modest increase during the winter at the sea ice edge and a stronger increase in a larger marginal ice zone during the summer. Increasing the sea ice albedo results in increased ice concentration or more compact ice pack, particularly during the summer melt season in the marginal ice zone.

The continuous application of the Ice911 material causes ice volume increase of (~0.5 to 1%/year). Sea ice volume increases are manifested in large-scale thickening of the ice pack in the case of the increased albedo experiment, ranging from 20 cm up to 1 m in increased ice thickness in the Canadian Archipelago.

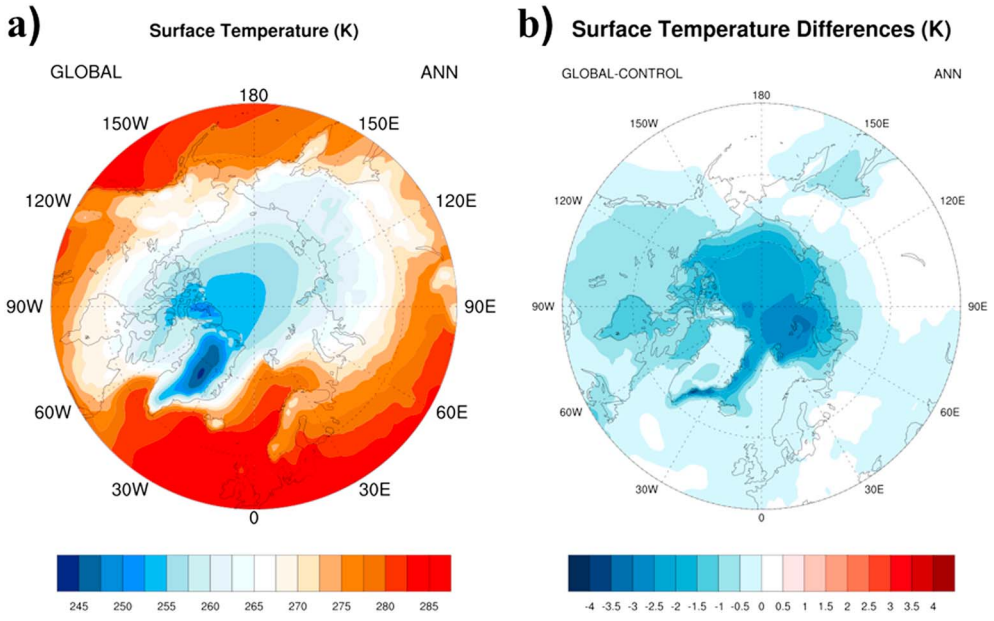

Figure 16. Surface temperature maps of (a) annual mean for Global albedo modification (b) difference in annual mean surface temperature between Global albedo modification and untreated Control.

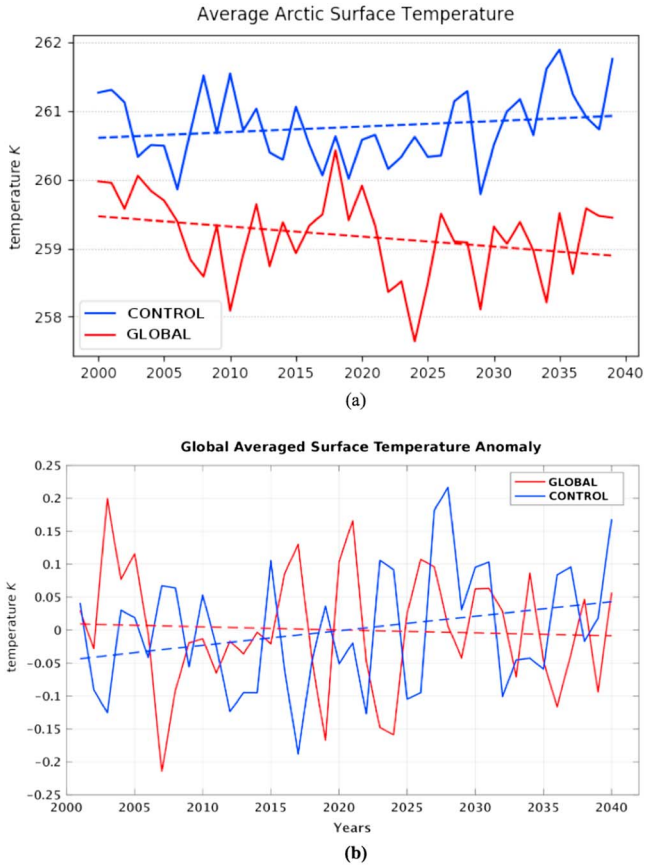

Figure 17. (a) Time series of Arctic annual mean surface temperature and (b) global averaged surface temperature interannual anomalies (with climatological mean removed) for Global albedo modification (red) and untreated Control (blue).

Climate modeling shows that a large part of Arctic sees more than 1.5°C cooler temperatures for global albedo modification as compared to the untreated control case. In a region north of the Barents and Kara Seas temperatures are reduced by 3°C and in North Canada by almost 1°C. From an analysis of the global average surface temperature anomalies trends, it is seen that over the period 2000–2040, the Control shows a 1°C rise in temperature, whereas the Global albedo modification case shows a modest decrease of 0.02°C over the same period. This demonstrates that global albedo modification could not only prevent the otherwise-expected 1°C rise in average global temperature but could further reduce the average global temperature by 0.02°C over the same period. These results are a promising indicator of the mitigation potential that exists from prospective technologies that are capable of enhancing surface albedo of sea ice over vast geographic areas.

An albedo enhancement in the Arctic is a relatively new idea that needs to be explored with further research. Let us discuss some of the pertinent issues about the set of experiments reported here and compare our results to standard benchmarks. Our simulation is initialized using GHG forcing from year 2000 using CESM compset "B_2000." Our study is in essence a perturbation experiment. We are comparing a relatively realistic Control (using the greenhouse forcing from year 2000) to our test case of enhanced Albedo (which is identical with the untreated control in every way except for the enhanced albedo). We have compared our Control to the PIOMAS (Schweiger et al., 2011, Zhang & Rothrock, 2003) data for the period 2000–2017 (see Figure 15). We note that the average sea ice volume time series in the control run shows a decreasing trend with time, in general, which is similar to that seen in the PIOMAS sea ice volume over the period 1980–2017.

It is worthwhile to briefly note here some of the other climate intervention technologies that are currently being explored as possible options. Bright hydrosols (Seitz, 2011), marine cloud brightening (Latham et al., 2012, 2014), blowing water over the Arctic sea ice (Desch et al., 2017), stratospheric aerosol injections, and experiments in GEOMIP (Kravitz et al., 2015; Tilmes et al., 2016) are some of the climate intervention technologies being reported in the recent literature. Seneviratne et al., 2018 reports a comparison of such technologies that may be grouped either as global solar radiation management (SRMglob) methods and regional land radiative management (LRMreg) methods with details of benefit and limitations for each method. The regional land radiative management described in Seneviratne et al. (2018) involves increasing the land surface albedo over HAA (Human-affected and affecting) regions. The global-scale temperature response from their experiment for such an application over the whole HAA regions is about 0.7°C particularly in the context of a 3.7°C warming for the 4 × CO_2 scenario, but negligible when only applied over single regions (see their Figure 2).

In order to quantify the changes in the temperature, ice area, and volume brought about by the albedo modification technique described here, we attempt to compare in particular to results from the CMIP5 set of emission-specific scenarios like the RCPs (see discussion in previous section). We note that our results are not directly comparable to the CMIP5 given the differences in the scenarios and metrics. However, a comparison from the IPCC AR5 report suggests that our Control simulation follows trends similar to RCP2.6; for example, our Control shows a 1°C increase in average global surface temperature between 2000 and 2040 (see IPCC AR5 report, http://ar5-syr.ipcc.ch/topic_pathways.php)). A similar comparison holds for the September sea ice extent between our Control and the RCP2.6 scenario reported in IPCC AR5. The global albedo enhancement in our Global experiment demonstrates a temperature mitigation potential of 1.02°C and sea ice volume mitigation of about 8% per decade during the period 2000 to 2040.

Some specific advantages of the Ice911 approach, and ice rebuilding efforts in general, are that it rebuilds a natural state of ice in the Arctic. If the treatment is discontinued, there is no predicted rebound effect. The

technology can be developed and studied with the aid of small, permitted field testing. The materials used in the Ice911 treatment are considered nontoxic, consisting of sand component silica, and in testing to date, they have shown no adverse impact on wildlife. The risks of an ice-free Arctic include the Arctic's contribution to increased world-wide temperatures through absorption rather than reflection of incoming summer-time solar radiation This in turn could lead to methane release from frozen permafrost reserves that are no longer protected by overlying Arctic sea ice. These serious climate risks are predicted to be greatly reduced by the restoration of thicker Arctic ice.

These advantages are in contrast to some apparent challenges that have been identified in some other proposed geoengineering techniques, such as the potential for damage to the ozone layer from deploying stratospheric sulfate aerosols for solar radiation management (see Seneviratne et al., 2018).

Simulating concurrent and continuous application of the Ice911 albedo enhancing material shows an immediate shift of the Arctic climate state to a thicker and colder Arctic. Using intelligent geoengineering (a repeating cycle of model, test, and monitor), with safe materials and a localized deployment, preliminary results indicate that a basin-wide albedo modification in the Arctic has potential to reduce climate change effects by thickening ice and lowering temperatures in the Arctic.

6. Future Work

Further study to establish the safety and risks of applying any material to restoring Arctic ice is needed. This includes further characterization of the ultimate fate of such added materials in polar environments—what proportion of the material sinks, floats, or dissolves over time is an area of active investigation by our team. While testing of the materials on fish and birds has shown no ill effects, evaluation of potential impacts by the materials on some further key species, such as marine mammals, needs to be done.

We also plan further work on deepening and quantifying our understanding of the albedo and thermal effects of the deployed materials on ice and snow. This could include addition of some periodic measurements using albedo sensors mounted on drones. We plan to incorporate redundant sensing architectures that prevent a single point of failure, which could, for instance, guard against the potential effects of a battery malfunction in a remote buoy. We also plan to include robust multisite data acquisition to gather more high-quality quantitative data on ice thickness, in addition to the data from image sensors, temperature strings, and manual readings of ice cores.

In addition, we want to conduct a thorough study through climate modeling to see if the process of increasing sea ice albedo in the Arctic and consequently increasing the sea ice pack and cooling down the temperature in Arctic could lead to any adverse climate effects anywhere in the world, particularly examining the impact of storm tracks and extreme weather events. As weather events have become more severe with the disappearance of much of the historic levels of multiyear ice in the Arctic, we need to explore through further climate modeling whether restoring ice in the Arctic could lead to a reduction of the severity of such extreme weather events.

Further work is planned for studying specific areas to propose for targeted treatments, areas that could be especially effective per unit area in preserving and restoring ice in the Arctic. Toward that end, our next step will be to model and simulate the targeted deployments of Ice911 materials over strategically chosen smaller areas in the Arctic and study their climate impacts. We seek areas that have a particularly large impact on ice restoration and cooling. In actual implementation of the Ice911 ice restoration geoengineering solution, starting with such areas would be of crucial importance from the standpoints of effectiveness, logistics, and cost minimization.

7. Modeling data

The link to the publicly accessible data that Climformatics used to generate the climate modeling plots in this paper is http://climformatics.com/earthsfuturepaper.tar.gz.

Acknowledgments
Ice911 is a registered 501(c)3 nonprofit, and wishes to express sincere thanks to all its individual, foundation, and corporate donors and supporters, its many volunteers, board members, advisory board members, and other key advisors. Special thanks go to the LaureL STEM Fund, The Mendelsohn Family Foundation, Barbara Grewen, and many other organizations and individuals for vital support. Without the contributions of these many individuals and organizations, this work could not have been done. We thank several corporations and nonprofits for key donations in kind and opportunities: Alaska Airlines, 3 M, Amazon Web Services, Covalent Metrology, Domino Data Lab, Google for Nonprofits, GSV Labs, Sustainable Silicon Valley, and the Truax Company, Inc. for a customized agricultural spreader. We thank the Cleantech Open, in which both Ice911 Research and Climformatics participated, resulting in many benefits, including meeting opportunities that led to the current collaboration. We thank IBM and Sabalcore for their generous donations of supercomputer time and administrative support and CESM-NCAR for use of their climate modeling tools. We thank Satish Chetty for expert instrumentation and deployment advice, Don Perovich and Phil Rasch for expert ice albedo and modeling advice, Peter Wadhams for his valuable insight into albedo observations, and Jim Haywood for kindly providing us valuable insights.

References

Briegleb, B. P., & Light, B. (2007). A delta-Eddington multiple scattering parameterization for solar radiation in the sea ice component of the Community Climate System Model (Tech. Note 472). Boulder, CO: National Center for Atmospheric Research.

Chetty, S. (2017). Linux powered autonomous Arctic buoys, Linux Open Source Summit and Embedded Linux Conference, Prague, Czechoslovakia, October 23, 2017.
Cvijanovic, I., Caldeira, K., & MacMartin, D. G. (2015). Impacts of ocean albedo alteration on Arctic sea ice restoration and Northern Hemisphere climate. *Environmental Research Letters*, *10*(2015), 044020.
Desch, S. J., Smith, N., Groppi, C., Vargas, P., Jackson, R., Kalyaan, A., et al. (2017). Arctic ice management. *Earth's Future*, *5*(1), 107–127. https://doi.org/10.1002/2016EF000410
Hurrell, J. W. M., Holland, M., & Gent, P. R. (2013). The Community Earth System Model. *Bulletin of the American Meteorological Society*. https://doi.org/10.1175/BAM%20S-D-12-00121.1
IPCC AR5 (2014). In C. B. Field, et al. (Eds.), *Climate change 2014: Impacts, adaptation, and vulnerability. Part A: Global and sectoral aspects. Contribution of Working Group II to the Fifth Assessment Report of the Intergovernmental Panel on Climate Change* (1132 pp.). Cambridge, UK and New York: Cambridge University Press. Retrieved from http://ar5-syr.ipcc.ch/topic_pathways.php
IPCC SR15 (2018). Climate Change 2014 Synthesis Fifth Assessment Report, Topic: 3 Future Pathways for Adaptation, Mitigation and Sustainable Development. Retrieved from http://www.ipcc.ch/report/sr15/
Kashiwase, H., Ohshima, K. I., Nihashi, S., & Hajo, E. (2017). Evidence for ice-ocean albedo feedback in the Arctic Ocean shifting to a seasonal ice zone. *Nature*, *7*, 8170. https://doi.org/10.1038/s41598-017-08467-z
Kravitz, B., Robock, A., Tilmes, S., Boucher, O., English, J. M., Irvine, P. J., et al. (2015). The Geoengineering Model Intercomparison Project Phase 6 (GeoMIP6): Simulation design and preliminary results. *Geoscientific Model Development*, *8*, 3379–3392. https://doi.org/10.5194/gmd-8-3379-2015
Latham, J., Bower, K., Choularton, T., Coe, H., Connolly, P., Cooper, G., & Craft, T. (2012). Marine cloud brightening. *Philosophical Transactions of the Royal Society A*, *370*(1974), 4217–4262.
Latham, J., Gadian, A., Fournier, J., Parkes, B., Wadhams, P., & Chen, J. (2014). Marine cloud brightening: Regional applications. *Philosophical Transactions of the Royal Society A*, *372*, 20140053.
IPCC AR4 (2007). Lemke, P., Ren, J., Alley, R. B., Allison, I., Carrasco, J., Flato, G., et al. (2007). Chapter 4: Observations: Changes in snow, ice and frozen ground, observations: Changes in snow, ice and frozen ground. In S. Solomon, et al. (Eds.), *Climate Change 2007: The Physical Science Basis. Contribution of Working Group I to the Fourth Assessment Report of the Intergovernmental Panel on Climate Change* (pp. 338–383). Cambridge, UK and New York: Cambridge University.
Meehl, G. A., Washington, W. M., Arblaster, J. M., Hu, A., Teng, H., Kay, J. E., et al. (2013). Climate change projections in CESM1(CAM5) compared to CCSM4. *Journal of Climate*, *26*, 6287–6308. https://doi.org/10.1175/JCLI-D-12-00572.1
Overland, J. E., & Wang, M. (2013). When will the summer Arctic be nearly sea ice free? *Geophysical Research Letters*, *40*, 2097–2101. https://doi.org/10.1002/grl.50316
Pistone, K., Eisenman, I., & Ramanathan, V. (2014). Observational determination of albedo decrease caused by vanishing Arctic sea ice. *PNAS*, *111*(9), 3322–3326.
Schweiger, A., Lindsay, R., Zhang, J., Steele, M., & Stern, H. (2011). Uncertainty in modeled arctic sea ice volume. *Journal of Geophysical Research*, *116*, C00D06. https://doi.org/10.1029/2011JC007084
Seitz, R. (2011). Bright water: Hydrosols, water conservation and climate change. *Climatic Change*, *105*, 365. https://doi.org/10.1007/s10584-010-9965-8
Seneviratne, S. I., Phipps, S. J., Pitman, A. J., Hirsch, A. L., Davin, E. L., Donat, M. G., et al. (2018). Land radiative management as contributor to regional-scale climate adaptation and mitigation. *Nature Geoscience*, *11*, 88–96. https://doi.org/10.1038/s41561-017-0057-5
Smedsrud, L. H., & Skogseth, R. (2006). Field measurements of Arctic grease ice properties and processes. *Cold Regions Science and Technology*, *44*(3), 171–183.
Stroeve, J. C., Kattsov, V., Barrett, A., Serreze, M., Pavlova, T., Holland, M., & Meier, W. N. (2012). Trends in Arctic sea ice extent from CMIP5, CMIP3 and observations. *Geophysical Research Letters*, *39*, L16502. https://doi.org/10.1029/2012GL052676
Taskjelle, T., Hudson, S., Granskog, M., Nicolaus, M., Lei, R., Gerland, S., et al. (2016). Spectral albedo and transmittance of thin young Arctic sea ice. *Journal of Geophysical Research: Oceans*, *121*, 540–553. https://doi.org/10.1002/2015JC011254
Tilmes, S., Sanderson, B. M., & O'Neill, B. C. (2016). Climate impacts of geoengineering in a delayed mitigation scenario. *Geophysical Research Letters*, *43*, 8222–8229. https://doi.org/10.1002/2016GL070122
Urrego-Blanco, J. R., Urban, N. M., Hunke, E. C., Turner, A. K., & Jeffery, N. (2016). Uncertainty quantification and global sensitivity analysis of the Los Alamos sea ice model. *Journal of Geophysical Research: Oceans*, *121*, 2709–2732. https://doi.org/10.1002/2015JC011558
Wadhams, P. (2017). *A farewell to ice: A report from the Arctic*. London, UK: Oxford University Press.
Zhang, J. L., & Rothrock, D. A. (2003). Modeling global sea ice with a thickness and enthalpy distribution model in generalized curvilinear coordinates. *Monthly Weather Review*, *131*, 845–861.

Erratum

The capital expense figures in the Supporting Information assume a 30 micron material diameter; this information was omitted from the originally published version of the Supporting Information. The following sentence has been added to the Supporting Information: "A commercially available version of the material with a 30-micron diameter and higher density is assumed for this targeted deployment calculation, to optimize required number of ships, logistics and cost." This may be considered the authoritative version of record.

Detelina Ivanova's affiliation was mistakenly listed as Scripps Institution of Oceanography, UCSD, but was accurately Climformatics, Inc. at the time the work was completed. This information has been updated and the corrected article may be considered the version of record.